

# Far-Infrared Herschel-PACS flux observations of OB stars

Rubio-Díez, M.M.<sup>1</sup>, Najarro, F.<sup>1</sup>, Traficante, A.<sup>2</sup>, Calzoletti, L.<sup>3,4</sup>, Puls, J.<sup>5</sup>, Herrero, A.<sup>6</sup>, Figer, D.<sup>7</sup>, Sundqvist, J.<sup>5</sup>, Trombley, C.<sup>7</sup> and Martin-Pintado, J.<sup>1</sup>

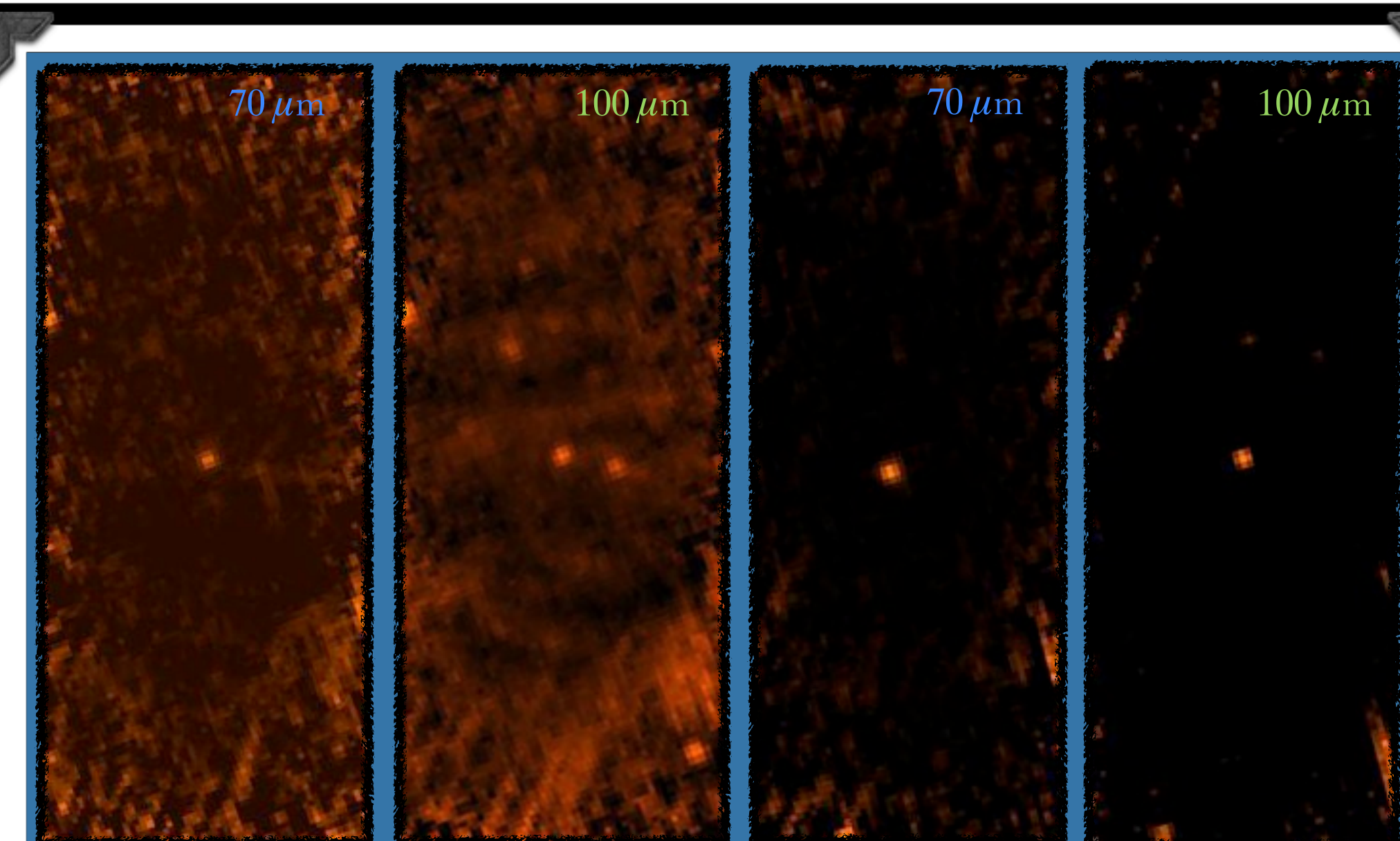
<sup>1</sup>Centro de Astrobiología, CSIC-INTA, Madrid (Spain); <sup>2</sup>Jodrell Bank Centre for Astrophysics, School of Physics and Astronomy, University of Manchester, Manchester (UK); <sup>3</sup>ASI Science Data Center, Roma (Italy); <sup>4</sup>INAF, Osservatorio Astronomico di Roma, Rome (Italy); <sup>5</sup>Universitäts-Sternwarte München, München (Germany); <sup>6</sup>Instituto de Astrofísica de Canarias, Tenerife (Spain); <sup>7</sup>Rochester Institute of Technology (RIT), NY (USA).



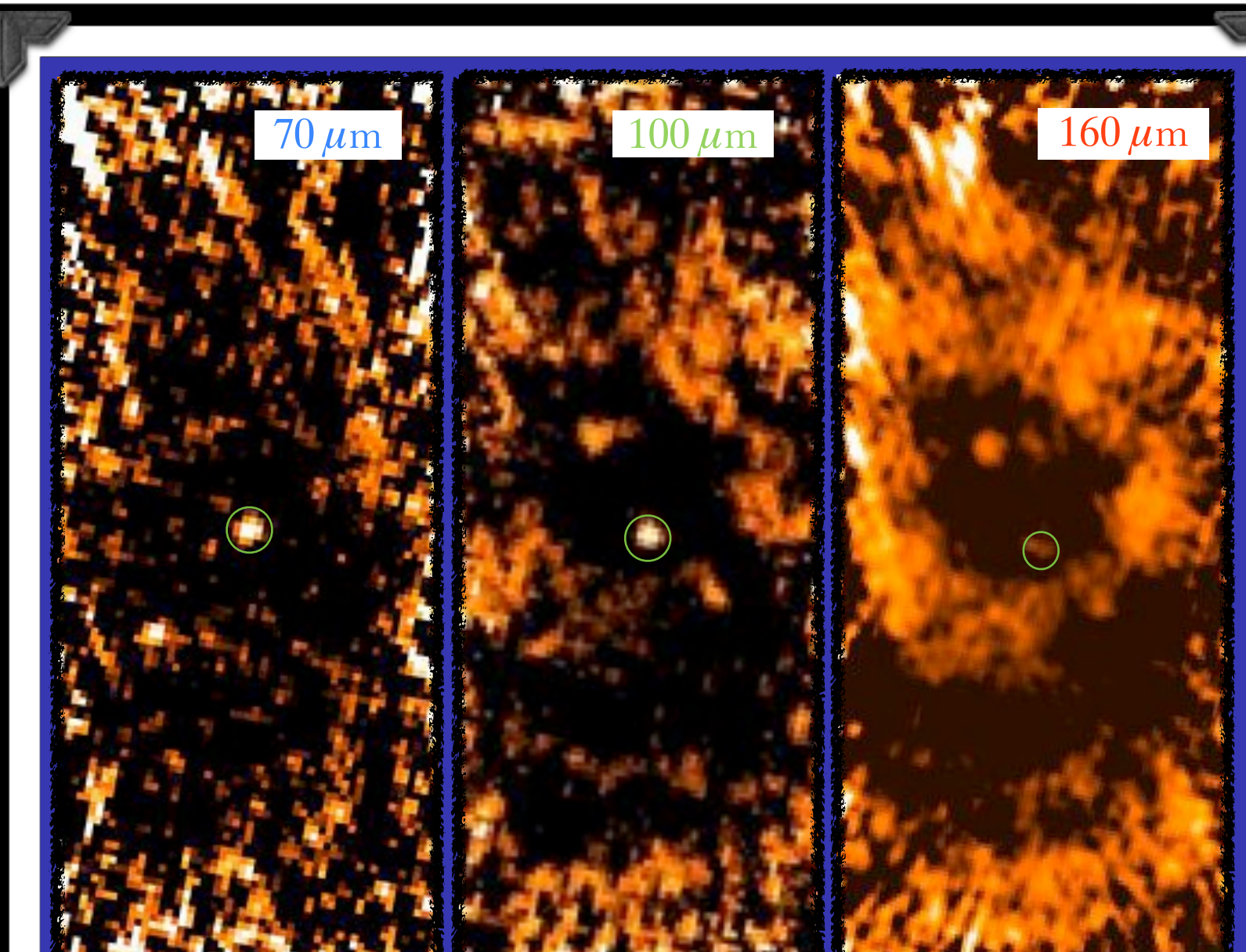
## Introduction

Mass-loss rates of luminous OB stars are inferred from different indicators, the strengths of UV P Cygni lines,  $H\alpha$  emission, and FIR and radio continuum emission. Studies taking into account small-density inhomogeneities (clumping) indicate that previously accepted mass-loss rates may need to be revised downwards. We argue that only a consistent treatment of ALL possible diagnostics, scanning different parts of the winds, and analyzed by means of state of the art model atmospheres, will permit the determination of true mass-loss rates.

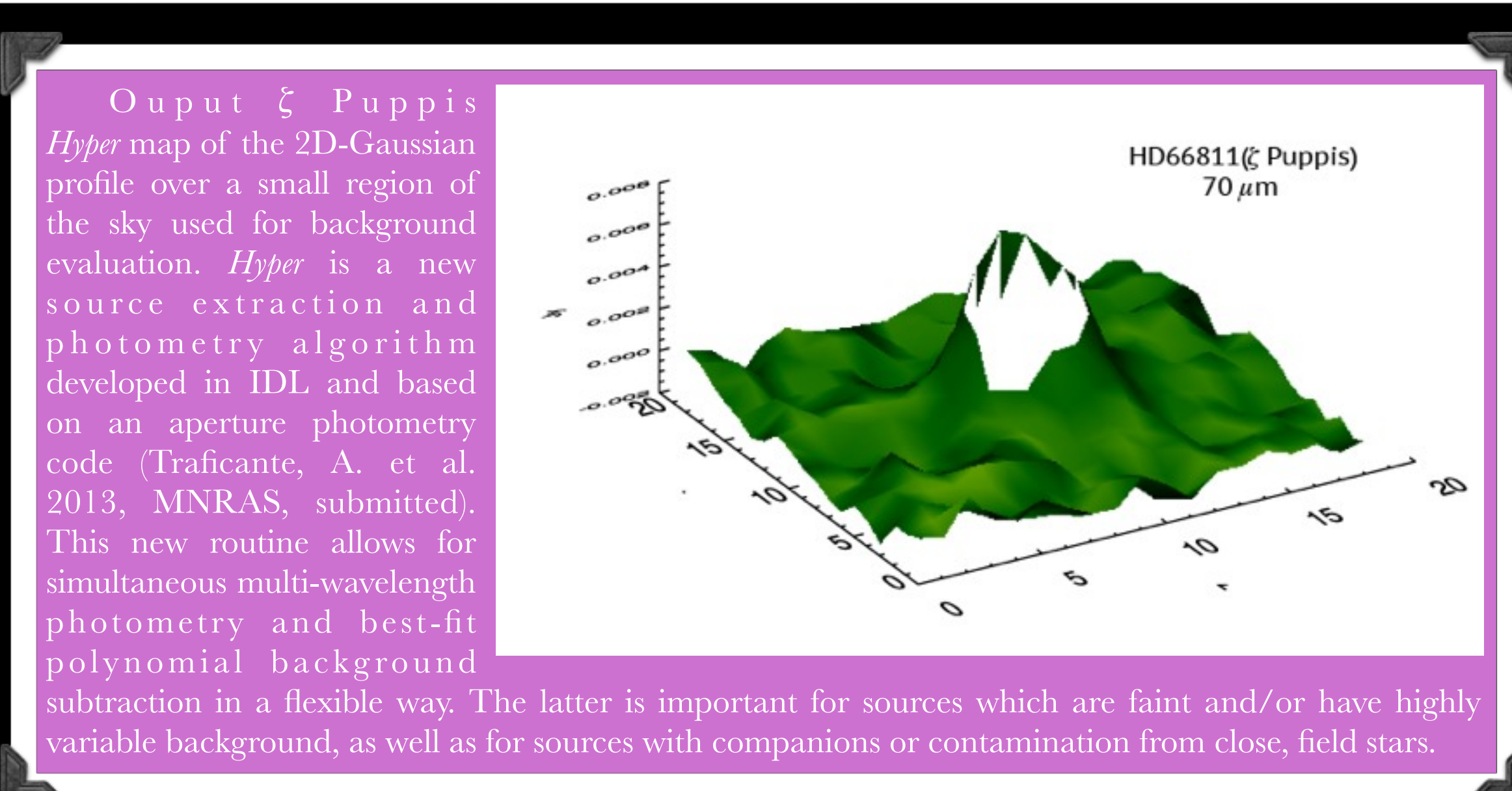
To this end we have assembled a variety of multi-wavelength data (optical, NIR and radio) of a carefully selected sample of 28 O4–B8 stars. However, one crucial observational set was missing: far-IR diagnostics of free-free emission, which uniquely constrains the clumping properties of the wind at intermediate wavelengths. We have used HERSCHEL-PACS photometric mode to fill this crucial gap, studying the 70 and 100 micron fluxes of our sample. These observations provide us with the missing information to derive the clumping properties of the entire outflow, allowing us to obtain reliable mass loss rates and improve our understanding of the wind physics. We present preliminary flux measurements at 70 and 100 micron and analysis of three objects of our sample of OB stars:  $\lambda$  Cep,  $\zeta$  Pup and  $\lambda$ 1 Ori.



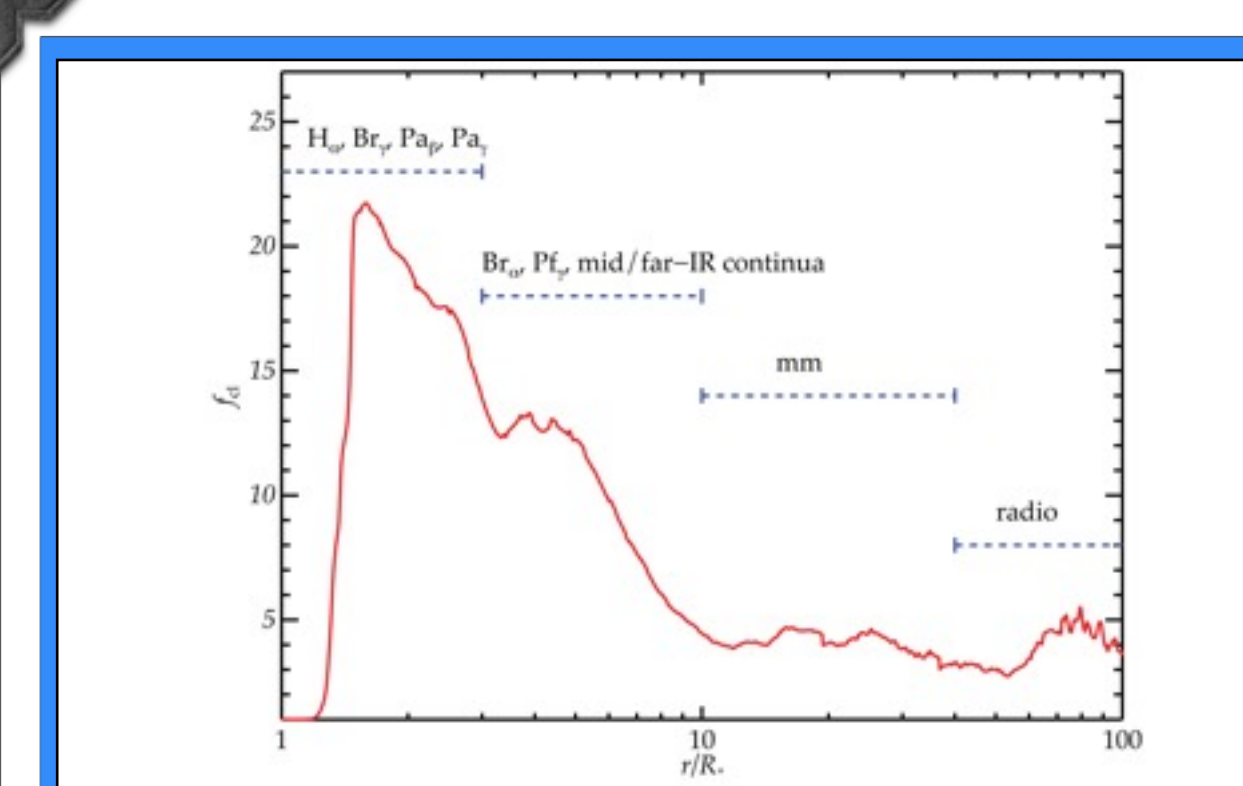
From left to right, scan maps at 70 and 100 micron of  $\lambda$  Cep and  $\zeta$  Pup, respectively. Resolution is 3.2 arcsec for a scan speed of  $20''/\text{pixel}$ . The maps were processed using PhotProject with the MMT deglitching method. Herschel/PACS also provided us with extra 160 micron observations of our sample. Unfortunately, just a few sources are barely detected at 160 microns, allowing us to determine only upper limits of the flux at that wavelength.



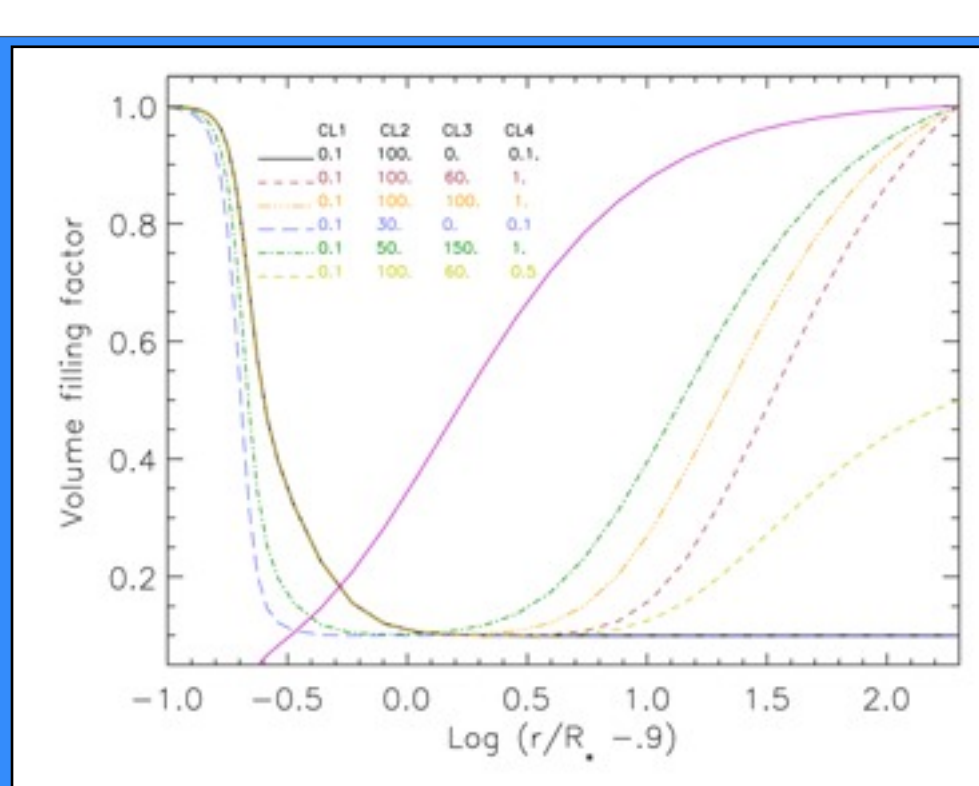
From left to right, PACS mini scan maps of HD154090 ( $\kappa$  Sco) at 70 ( $3.2''$ ), 100 ( $3.2''$ ) and 160 ( $2''$ ) micron, respectively. The maps were reduced using PhotProject with MMT deglitching method. Unexpectedly, the star still is visible and a ring structure was detected at the longest wavelengths.



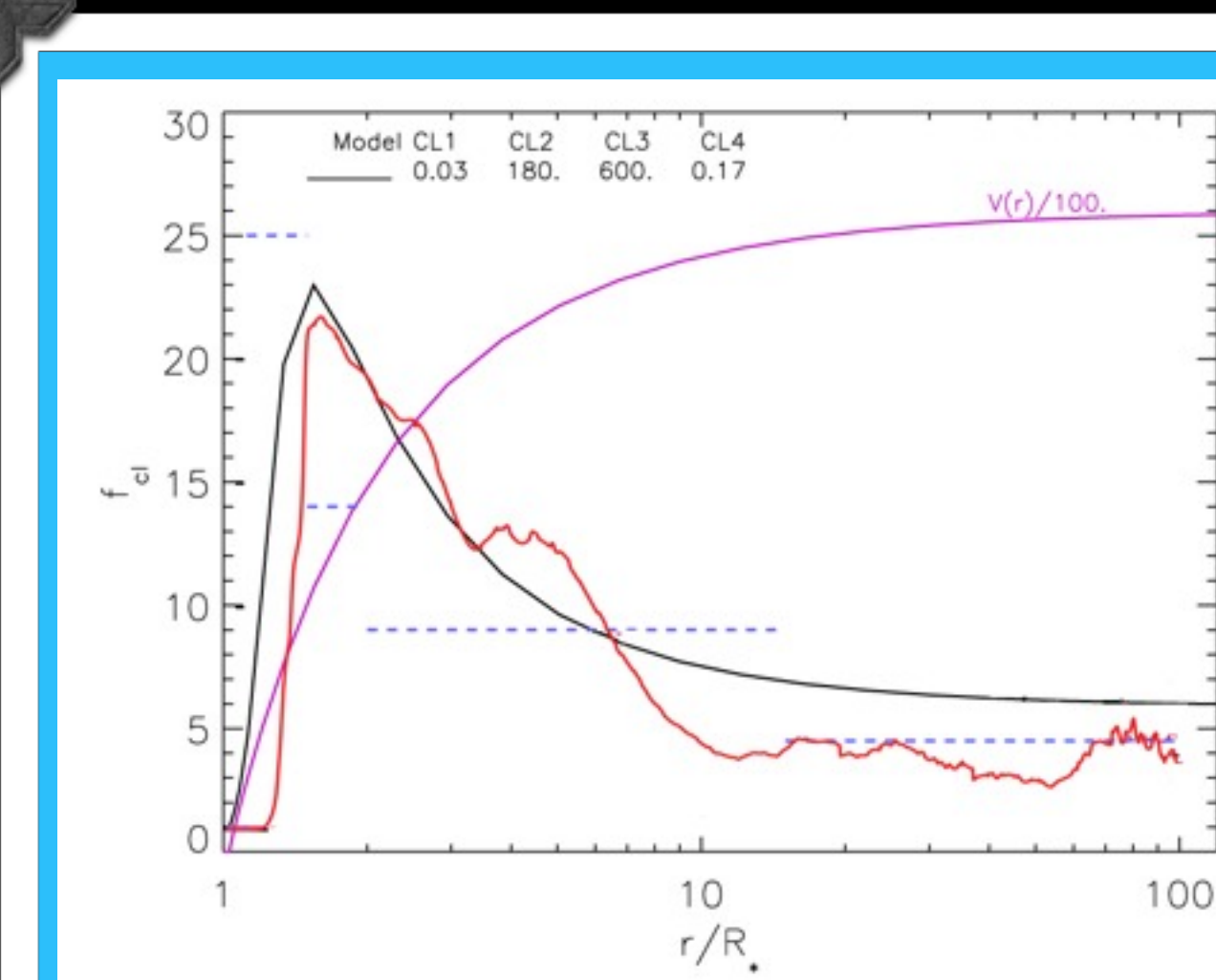
**Output  $\zeta$  Puppis**  
*Hyper* map of the 2D-Gaussian profile over a small region of the sky used for background evaluation. *Hyper* is a new source extraction and photometry algorithm developed in IDL and based on an aperture photometry code (Traficante, A. et al. 2013, MNRAS, submitted). This new routine allows for simultaneous multi-wavelength photometry and best-fit polynomial background subtraction in a flexible way. The latter is important for sources which are faint and/or have highly variable background, as well as for sources with companions or contamination from close, field stars.



The volume filling factor,  $f_v$ , is the fractional volume of the dense gas:  
 $\langle \rho \rangle = f_v \rho^+$ ,  $\langle \rho^2 \rangle = f_v \langle \rho^+ \rangle^2$ , where  $\rho^+$  is the density inside the overdense clumps and  $\langle \rho \rangle = M/(4\pi r^2 v)$ .  
The clumping factor,  $f_{cl}$ , describes the overdensity of the clumps:  $f_{cl} = \langle \rho \rangle / \langle \rho^+ \rangle$  with  $f_{cl} = f_v^{-1}$  and  $\rho^+ = f_{cl} \langle \rho \rangle$ .  
Here, radial stratification clumping-factor from one of the models in Sundqvist &



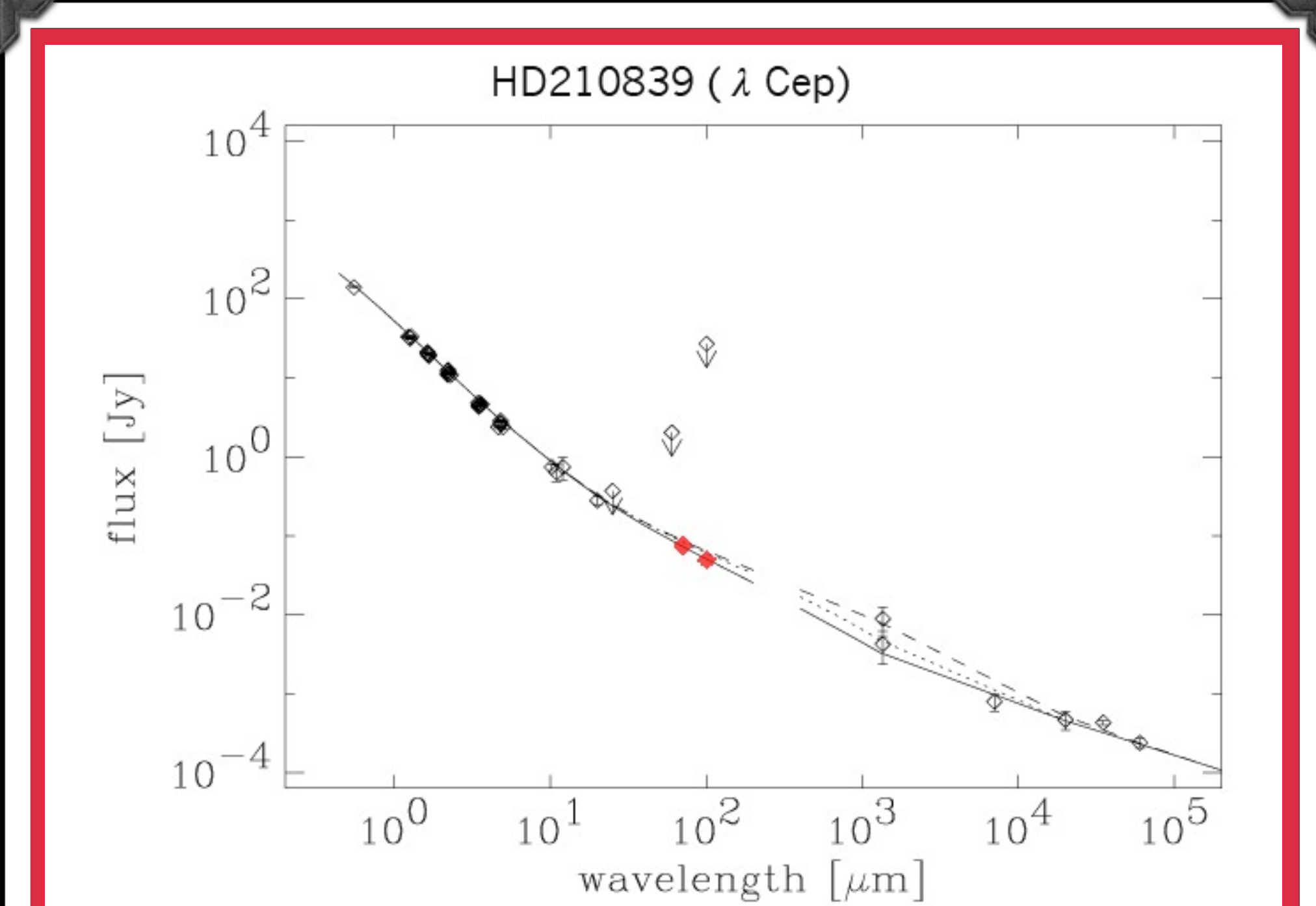
Another way of characterising the clumping is through the radial stratification of the volume filling factor,  $f_v$ , introduced by Najarro et al. (2009, ApJ, 691, 1816):  
 $f_v(r) = CL_1 + (1 - CL_1) e^{-(v(r)/CL_2)} + (CL_1 - CL_1) e^{-(v(r)-v_{out})/CL_3}$   
Left: examples for the radial structure of the volume filling factor,  $f_v(r)$ , for different values of  $CL_{1,2,3,4}$ . The wind velocity structure is displayed in magenta.



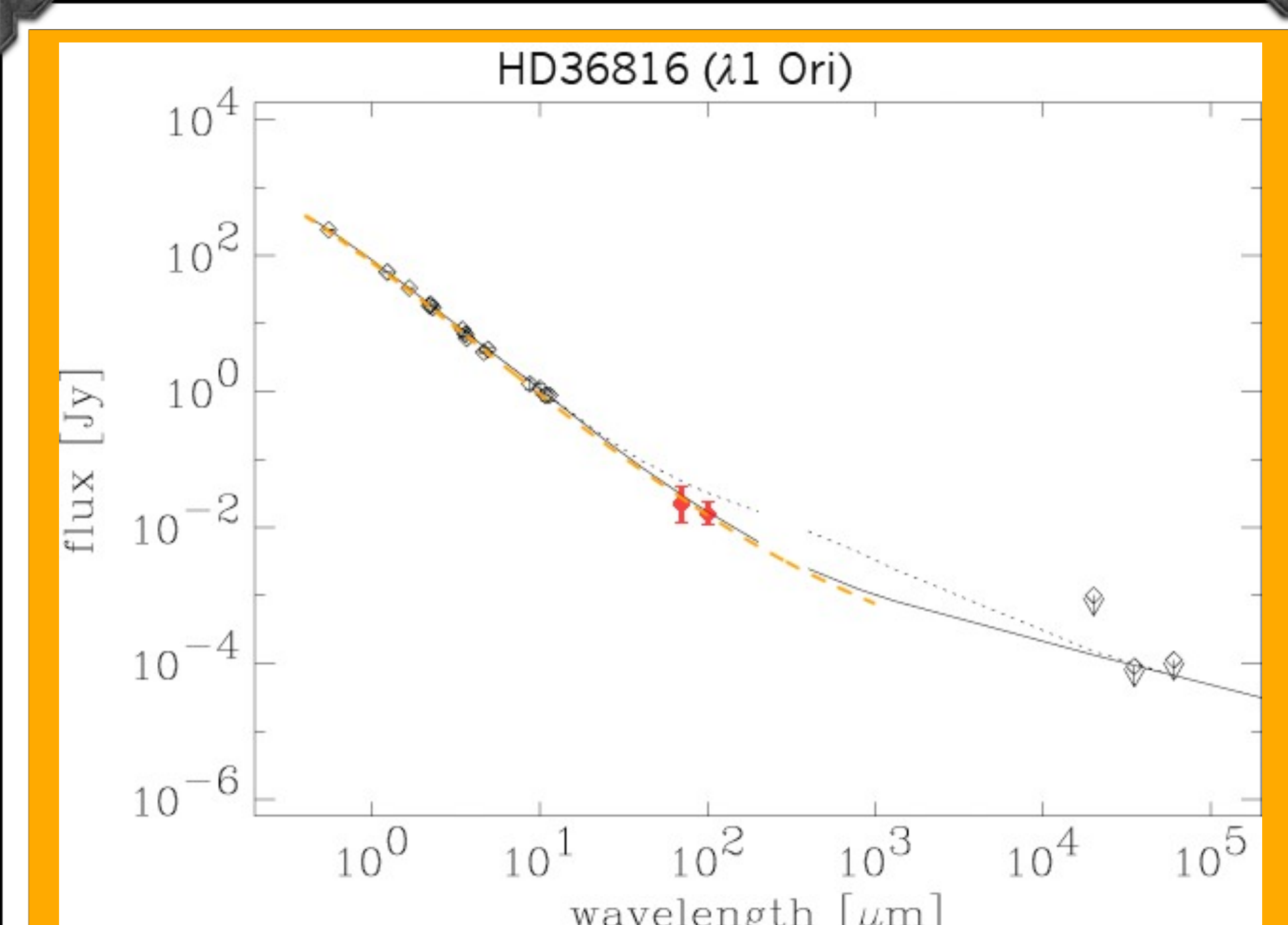
Radial stratification of the clumping factor,  $f_{cl}$ , for  $\zeta$  Pup. Black solid: clumping law derived from our model fits (adapted from Najarro et al. 2011, A&A, 535, 32), where  $f_{cl} = 1/f_v$ . Red solid: Theoretical predictions of the clumping factor by Sundqvist & Owocki (2013) from a radiation-hydrodynamical line-driven instability simulation including limb darkening and a sound-wave perturbation at the photospheric base.

Dashed: Average clumping factors for different regions,  $f_{cl}^{in}$  [ $r_{in}$ ,  $r_{mid}$ ],  $f_{cl}^{mid}$  [ $r_{mid}$ ,  $r_{out}$ ],  $f_{cl}^{out}$  [ $r_{out}$ ,  $r_{far}$ ],  $f_{cl}^{tot}$  ( $> r_{far}$ ), derived by Puls et al. (2006, A&A, 454, 625) assuming an outer wind with clumping as theoretically predicted. Typical values are  $r_{in}=1.05$ ,  $r_{mid}=2$ ,  $r_{out}=15$  and  $r_{far}=50 r/R$ . Magenta solid: run of the velocity field in units of  $100 \text{ km s}^{-1}$ .

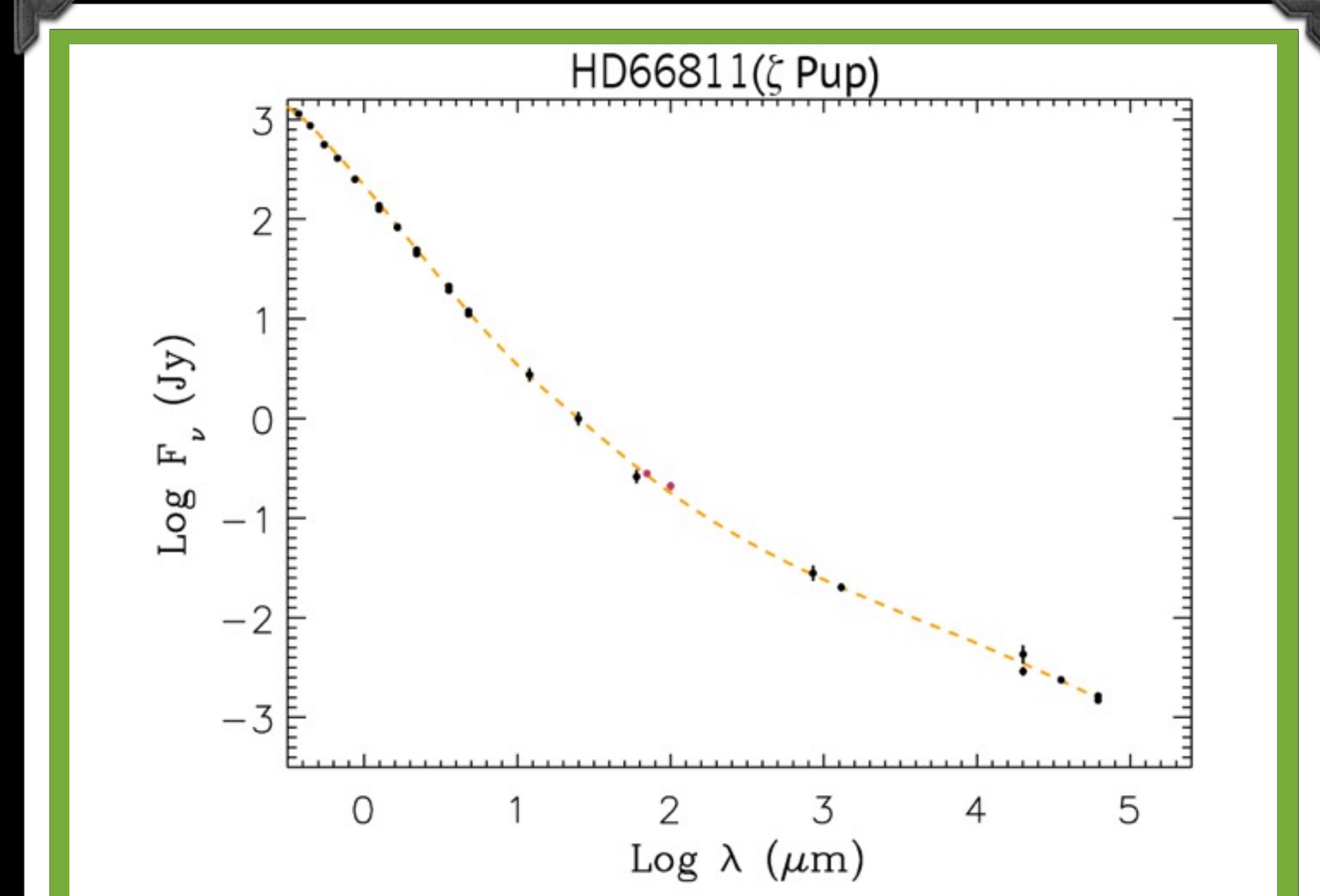
Owocki (2013, MNRAS, 428, 1837). The formation regions of different diagnostics are indicated.



Clumped models ( $f_{cl}^{in}=f_{cl}^{mid}=6.5$ ,  $f_{cl}^{out}=1$ , solid;  $f_{cl}^{in}=6.5$ ,  $f_{cl}^{mid}=10$ ,  $f_{cl}^{out}=1$  and  $f_{cl}^{out}=8$ , dotted and dashed, respectively) for  $\lambda$  Cep compared to the IR/radio continuum fluxes adapted from Puls et al. 2006 (A&A 454, 625). Red rhombus correspond to our PACS fluxes of the star at 70 and 100  $\mu\text{m}$  (error bars are smaller than the symbols). Our measurements slightly constrain the clumping at intermediate wavelengths, pointing to a weak clumping structure in the outer region.



Minimum and maximum clumped models ( $f_{cl}^{in}=2$ ,  $f_{cl}^{mid}=1$ , solid line;  $f_{cl}^{in}=4$ ,  $f_{cl}^{mid}=20$ , dotted line) for HD36816 compared with the IR/radio continuum measurements (Puls et al. 2006, A&A, 454, 625). Overplotted, the red symbols represent PACS fluxes of the star at 70 and 100  $\mu\text{m}$ , while yellow dashed line indicates the unclumped model of the emergent flux of the star using the mass-loss rate from Br $\gamma$  (Najarro et al. 2011, A&A, 535, 32). Our far-infrared observations clearly disentangle the uncertainty in the clumping models and point to low clumping in the intermediate region.



Best clumped model of emergent flux for  $\zeta$  Pup,  $CL_1=0.03$ ,  $CL_2=180$ ,  $CL_3=600$  and  $CL_4=0.17$  (adapted from Najarro et al 2011, A&A, 535, 32). Black circles represent the IR/radio continuum archival measurements. Red circles correspond to our PACS fluxes of the star at 70 and 100  $\mu\text{m}$ . Note how these new flux values agree very well with the derived clumping structure,  $f_{cl} = f_{cl}^{-1} = 0.03$ .

## Preliminary Results

In addition to the results of the photometric fluxes, we have performed a preliminary analysis of the three O giant and supergiant stars of our sample:

**$\lambda$  Cep**: The new photometric flux values of this star are consistent with the three different clumping models compared to the IR/radio continuum fluxes (Puls et al. 2006, A&A, 454, 625). Although our measurements might indicate a weak outer wind, the two different SCUBA fluxes measured at 1.35mm and the gap at 100-1000 microns makes it difficult to discern between models.

**$\lambda$ 1 Ori**: Interestingly, flux values at 70 and 100  $\mu\text{m}$  perfectly match, at IR wavelengths, with our unclumped model computed with the mass-loss rate measures in Br $\gamma$  (Najarro et al. 2011, 2011, A&A, 535, 32). This result confirms one of the two possible solutions found by Puls et al. 2006 (A&A, 454, 625) for this star ( $f_{cl}^{in}=2$ ,  $f_{cl}^{mid}=1$ ,  $f_{cl}^{out}=1$ ).

**$\zeta$  Pup**: Our observations agree very well with our clumping model simulation of IR to radio continuum, using as input the volume filling factor,  $f_v = f_{cl}^{-1}$ , calculated by Najarro et al. (2011, A&A, 535, 32) via spectroscopic analysis of L and K bands.

Our preliminary analysis of far-IR fluxes compared with previous clumping model simulations for some sources shows the importance of multi-wavelength observations to derive the clumping properties of the entire outflow, in order to better understand the wind physics and to obtain reliable mass-loss rates of OB stars.